

Performance evaluation of optical network-on-chip based on MIMO system

SOFIEN MHATLI^a, BECHIR NSIRI^b, MALAK CHANNOUFI^{a,c}, MUTSAM A.JARAJREH^d, MOHAMMAD GHANBARISABAGH^e, LAXMAN TAWADE^f, RABAH ATTIA^a

^aSERCOM-Labs, EPT Université de Carthage, 2078, La Marsa, Tunis, Tunisia

^bSys'com Lab, ENIT, BP.37 Le Belvédère 1002Tunis, Tunisia

^cETIS-ENSEA-UMR 8051, University of Cergy-Pontoise, France

^dFaculty of Engineering & Environment, Northumbria University, Ellison Place, Newcastle upon Tyne, NE1 8ST, UK

^eSchool of Computer and Communication Engineering, University Malaysia Perlis, Pauh Putra, 02600 Perlis, Malaysia

^fElectronics and Telecommunication Department VDF School of Engineering and Technology, Latur, India

When designing Optical Networks-On-Chip, designers have resorted to make dialogue between emitters (lasers) and receivers (photo-detectors) through a waveguide which is based mainly on optical routers called λ -router. In this document, we propose a new method based on the multiple concepts of Inputs and Output, and we give a model of the channel propagation, then we discuss the MIMO CDMA systems to assess its performance. For this we present the family of code used and we develop the receiver algorithm of such systems. Finally, we present simulations to validate the presented system.

(Received April 19, 2014; accepted July 10, 2014)

Keywords: ONOC, MIMO, diffusers, VBLAST, OCDMA

1. Introduction

As we progress towards more advanced technologies and lower transistor dimensions, power is the main constraint which will mandate the architecture of future systems. Hence, our optimization problem is how to get the most performance within the power envelope determined by the application. Ideas like dynamic power management of the system [1] or putting more cache [2] have been proposed.

These kinds of solutions come with a performance cost which makes them less attractive. Hence, it is obvious that more transformational solutions are needed. Hence, researchers opt for optics as an alternative; one of the more mature technologies for interconnects.

Electrical interconnects have long been used in on-chip communication. They are CMOS compatible, have high integration density, and when repeated have high signal integrity. Moreover, electrical interconnects have been known for their high performance and low power. However, as we march towards the new fabrication technologies, electrical interconnects are not scaling.

On-chip optical interconnects are viewed as a potential replacement for electrical interconnect. Among the emerging technologies, it is considered the most mature [3]. The optical interconnects hold several advantages over traditional copper interconnects as discussed by Beausoleil et al. [4, 5, 6].

The main advantages could be summarized as follow: Light speed latency, high bandwidth and low power.

Photonic Network-on-Chip (NoC) architectures are emerging as a new paradigm to interconnect a large number of processing cores at chip level, meeting the pressing demand for extremely high bandwidth and low power consumption. Optical routers, which are typically composed of silicon waveguides and optical switches, play a key role in an on-chip photonic interconnection network.

ONoC has been considered to enabling high bandwidth and low contention routing of data [7] using wavelength division multiplexing (WDM)-enabled optical waveguides [8]. In [9] optical switch and waveguides [10] are used in ONoC to realize the same function as a conventional electrical router but with routing based on wavelength and with no need for an arbiter [11].

In [12], a micro-network architecture based on wavelength routing is suggested for on-chip optical networks, this architecture has been generalized in [13] and the routing scheme for this architecture is also developed.

Instead of wavelength routing based on optical switch which is the main research interest in ONOC system, we opt in this paper to a free space channel between source nodes and destination nodes, and the routing scheme is based on OOC code.

In this study, we focus on a new architecture on ONOC which is based on MIMO CDMA techniques and free space channel for the first time. Indeed, there's no previously work in the applications of MIMO techniques in ONOC system and routing between source nodes and receiver nodes.

We present here an overview of On-chip optical networks based on (λ -router). The figure below shows an example of a network-on-chip based on an optical waveguide using optical router architecture liabilities (the λ -router) [14, 15].

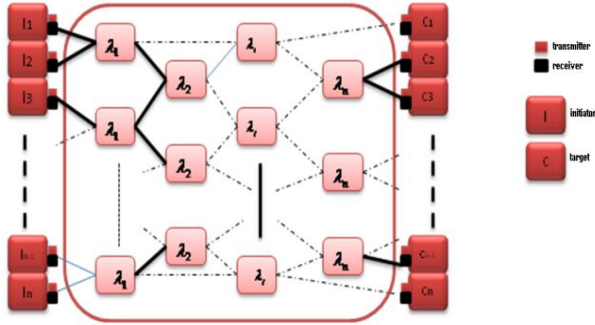


Fig. 1. On-chip optical networks based on λ -router.

The basic element of the network is the λ -router [16] which consists of two basic elements:

- * Two parallel waveguides.
- * A ring cavity, square...

Our idea is to replace the propagation channel based on the micro resonator by a free space to ensure a more secure and reliable communication in terms of throughput. For this, we have implemented channel propagation in free space for communication between different chips.

In this paper, we will study a novel ONOC (Optical Network on Chip) system based on MIMO technology; we begin in section II by modeling the propagation's system channel which allows us to determine the attenuation between transmitter and receiver and then the channel coefficients. Then in section III, we present the study of ONOC system based on MIMO CDMA technology, and finally, in section IV, numerical results are presented.

2. MIMO channel modeling

To ensure communication between different transmitters and receivers we used the optical diffuser to ensure the dissemination of the laser signal to all receivers.

In this section, we solve Maxwell's equations to determine the electromagnetic field equation that describes the outgoing laser light [17] and we model the diffuser which is a significant component to diffuse light to all receivers.

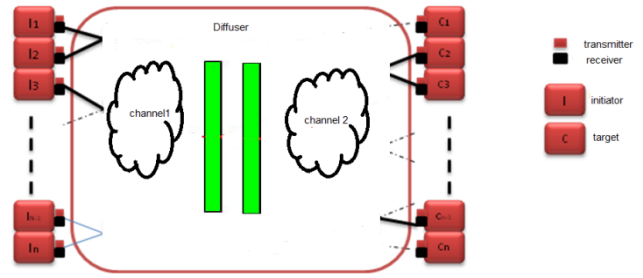


Fig. 2. On-chip optical networks based on MIMO technology.

A. Channel 1 modeling

We assume that electromagnetic wave Propagates in a homogeneous medium is subject to Maxwell's equations. Thus, the equation of wave propagation in isotropic medium is:

$$\Delta \vec{E} - \frac{1}{c^2} \frac{\partial^2 \vec{E}}{\partial t^2} = \vec{0} \tag{1}$$

If we consider the propagation of a monochromatic electromagnetic wave frequency, then we have:

$$\Delta E(x, y, z) + k^2 E(x, y, z) = 0 \tag{2}$$

Where $k = \frac{2\pi}{\lambda}$ is the wave number, where λ is the wavelength of the materiel where the beam propagates.

The solution of this equation is the Amplitude distribution of a Gaussian laser beam can be written as in [18].

$$I(r, z) = I_0(z) \exp\left(\frac{-2r^2}{w^2(z)}\right) \tag{3}$$

Where

$$w(z) = w_0 \sqrt{1 + \left(\frac{z}{z_R}\right)^2}$$

Describes the evolution along

the propagation direction of the points having a decrease of $\frac{1}{e}$ and r is a transversal dimension.

The width, the local divergence, and the radius of curvature contain a special dependence with w_0 and λ . This dependence can be written in the form of length that is defined as: $z_R = \frac{\pi w_0^2}{\lambda}$ This parameter is known as the Rayleigh range of the Gaussian beam. Its meaning is

related to the behavior of the beam along the propagating distance.

w_0 is the beam waist width when $z=0$.

The percentage of energy F received by the receiver is defined by:

$$F = \frac{\int_0^{\rho} I(r) ds}{\int_0^{\infty} I(r) ds} \quad (4)$$

With $dS = 2\pi.r.dr$

If we replace $I(r)$ by its Gaussian expression, we obtain after simplification

$$F = \frac{\int_0^{\rho} r e^{-2\frac{r^2}{w^2}} dr}{\int_0^{\infty} r e^{-2\frac{r^2}{w^2}} dr} \quad (5)$$

We can easily calculate this integral (using the variable $t=r^2$):

$$\int_0^{\rho} r e^{-2\frac{r^2}{w^2}} dr = \frac{1}{2} \int_0^{\rho^2} e^{-2\frac{t}{w^2}} dt = \frac{1}{2} \left[-\frac{w^2}{2} e^{-\frac{2t}{w^2}} \right]_0^{\rho^2} \quad (6)$$

Finally we find:

$$F = 1 - \exp\left(-2\left(\frac{\rho}{w}\right)^2\right) \quad (7)$$

B. Channel 2 modeling

As lasers scatter light linearly, the diffuser appears as a solution to distribute the quantity of light received at the receivers, in this case we say that the diffusion process is done in a Lambertian.

Existing diffusers are either single surface or double surfaces [19,20].

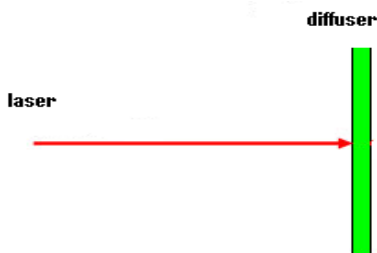


Fig. 3. Diagram of a diffuser.

The diffuser is an optical component, composed of several different micro-lenses, designed in a manner that each micro-lens arranged to avoid repetition pattern, so that there's control over the distribution of diffusion and intensity profile [20].

For each diffuser:

$$I_0(\theta) = \begin{cases} \cos^p\left(\frac{\pi}{2} \frac{\theta}{\theta_0}\right), & |\theta| \leq \theta_0 \\ 0 & \text{otherwise} \end{cases} \quad (8)$$

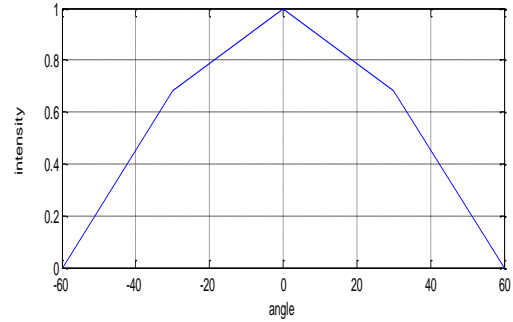


Fig. 4. Response of a diffuser.

In our study we choose $\theta_0 = 60^\circ$ (angular spread of the diffused signal) and $p = 0.6$ (shape fitness) which is the parameters of a commercial available diffusers.

It is a simple diffuser with low spectral efficiency [19]. In order to increase the spectral efficiency we adopt the use of two broadcasters which are placed one in front of the other as shown in the following figure.

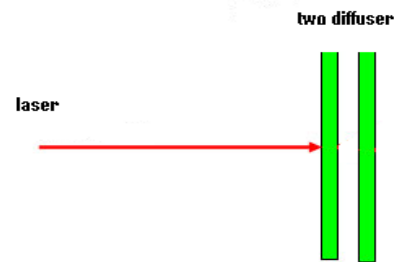


Fig. 5. Diagram of two diffusers.

The total scattering given by two broadcasters is given by the convolution product:

$$I(\theta) = \int_{-90}^{90} I_0(\varphi) I_0(\theta - \varphi) d\varphi \quad (9)$$

In our study we choose $\theta_0 = 60^\circ$ and $p = 0.6$

The spectral efficiency is 70% [19] and there is an increasing scattering angle going from 120° to 180° .

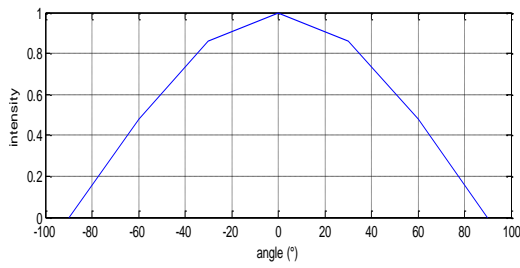


Fig. 6. Response of two diffusers.

Then, the channel 2 is represented with:

$$h_{ij} = \frac{A}{d_{ij}^2} I(\theta) \cos(\varphi_{ij}) \quad (10)$$

h_{ij} : The coefficient of the ONOC channel.

3. Study of ONOC MIMO CDMA architecture

Instead of wavelength routing based on optical switch, we opt in this paper to a free space channel between source nodes and destination nodes. So, to ensure the communication between the transmitter and the dedicated receiver we use the multiple access code division (CDMA) technology which is widely used in the radio frequency domain where it provides multiple access and share resources in a flexible and reconfigurable. The spread spectrum allows secure transmission. However, the problem encountered when using the CDMA multiple access technique as is the choice of the code sequences to be used as a signature of different transmitters.

In the first part, we present the transmission of a MIMO CDMA optical system as well as the study of the reception part with the introduction of the dedicated algorithm for reception. Finally, we evaluate the performance of the system with simulated bit error rate as a function of signal to noise ratio.

C. Transceiver part

In a ONOC MIMO CDMA system user data are spread by multiplication with a code sequence.

The following figure shows a simplified diagram of the transmission part of CDMA optical network based on electrical encoders.

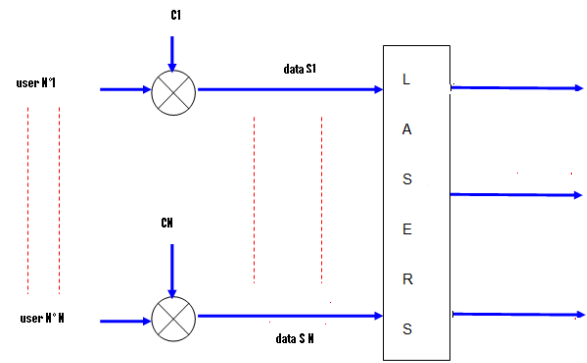


Fig. 7. The transceiver part.

Optical orthogonal codes (OOC) have been presented in 1989 by Al Salehi to solve problems by using, in the optical domain, bipolar sequences and coherent system [22] detection. Note that in the case of OOC, the generation of code words to form a family of sequences applicable to optical CDMA is exhaustive.

The construction of OOC codes "strict" is based on the control of the position of each chip in a given code sequence [22]. The position of the chip depends on that of the other chips in the same sequence of 1, and the positions of the chips 1 to code sequences belonging to the same family.

A code is called "strict" OOC if it meets the following criteria [24, 25, and 26].

The total length L of a sequence of OOC "strict" code should be equal to $L = 2D + 3$, knowing that D is the maximum distance between the first and last non-zero chip code sequences belonging to the same family.

We present in Table 1 few examples of families OOC code "strict".

Table 1. Example of OOC codes.

N	L	G	$C_i = \{b_1^{(i)}, b_2^{(i)}, b_3^{(i)}\}$
3	21	3	C1={1,2,6}; C2= {1,3,9}; C3={1,4,11};
2	29	4	C1={1,2,8,12}; C2= {1,3,6,15};
4	57	4	C1={1,2,12,25}; C2= {1,5,22,25}; C3={1,4,20,29};

The code sequence is the signature of each user. It should allow to easily distinguishing the desired user from other users.

The autocorrelation value λ_a and the cross-correlation value λ_c are the key parameters to optimize system performance in the presence of multiple users.

Autocorrelation: describes the degree of similarity between the code and its shifted version. The higher the

value, the more it will be possible to differentiate the desired code in a staggered version of this code.

Cross-correlation: measure the degree of similarity between the code and the other families of codes. The higher the value, the more it will be possible to differentiate the desired code other family codes.

We consider two different users codes $c_k(t)$ and $c_i(t)$:

The correlation function:

$$|Z_{c_i, c_k}(l)| = \left| \sum_{j=1}^F c_{i,j} c_{k,j+l} \right| = \begin{cases} W & \text{for } l=0 \\ \leq \lambda_a & \text{for } 1 \leq l \leq F-1 \end{cases} \quad (11)$$

The cross-correlation function:

$$|Z_{c_i, c_k}(l)| = \left| \sum_{j=1}^F c_{i,j} c_{k,j+l} \right| \leq \lambda_c \quad \text{for } 1 \leq l \leq F-1 \quad (12)$$

The autocorrelation function curve of codeword (1,2,6) and the cross-correlation function curve between it and codeword (1,3,9) in (21,3,1)-OOC are shown in this figure.

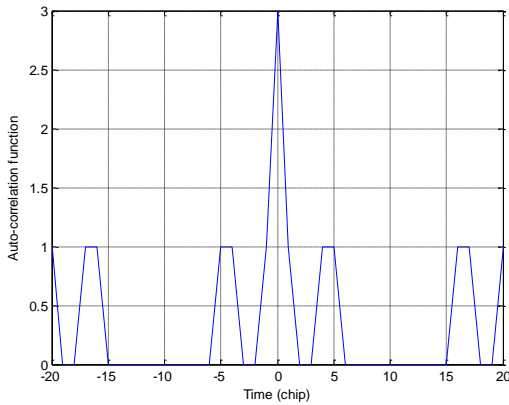


Fig. 8. Auto-correlation function of codeword (1, 2, 6).

The result shown in Fig. 8 that autocorrelation is respected and $\lambda_a \leq 1$.

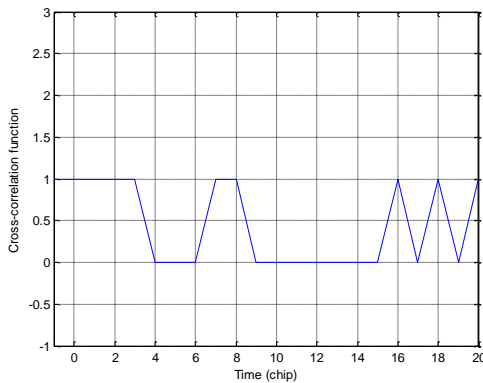


Fig. 9. Cross correlation between codeword (1, 2, 6) and (1, 3, 9).

The result shown in Fig. 9 that autocorrelation is respected and $\lambda_c \leq 1$.

The K^{th} user data are multiplied by the code that he

associates. At the output of the encoder, we obtain the following signal [26]:

$$s_k = b_k(t)c_k(t) \quad (13)$$

$b_k(t)$ Represent the data of the same user.

$$b_k(t) = \sum_{i=-\infty}^{\infty} b_i^{(k)} P_{T_b}(t - iT_b) \quad (14)$$

$b_i^{(k)}$ is the i^{th} bit of user data theme, takes the value 0 or 1 with equal probability.

$P_{T_b(t)}$ is a rectangular pulse of duration.

$D = 1/T_b$ is the bandwidth of the k^{th} user.

$c_k(t)$ is the sequence of the k^{th} user code.

$$c_k(t) = \sum_{j=-\infty}^{\infty} c_j^{(k)} P_{T_c}(t - jT_c) \quad (15)$$

$P_{T_c}(t)$ is the rectangular pulse of duration T_c , called "chip time".

$c_j^{(k)}$ is the j^{th} element called "chip" of the k^{th} user code.

The code sequence $c_j^{(k)}$ for j from 0 to $L-1$ is a periodic

sequence of period L as $L = \frac{T_b}{T_c}$

Where $D_c = \frac{1}{T_c}$ is the "chip rate" as $D_c = LD$.

At the transmitter output and the receiver input, the signal $r(t)$ is the superposition of the signals emitted by the N users, which are influenced by the MIMO channel:

$$r(t) = \gamma P_{laser} \sum_{i=1}^{i=N_i} h_{ij} s_i(t - \tau_i) + \sqrt{i_{nj}^2} \quad (16)$$

With:

γ : Receiver sensitivity.

i_{nj}^2 : The average noise power.

τ_k : Represents the delay of the k^{th} user.

h_{ij} : The coefficient of the ONOC channel calculated in section II, after the conception of the channel transfer function between source nodes and receiver nodes.

During the simulations, we generated random numbers with Gaussian statistics for the modeled noise is added to the received signals.

D. reception part

In the reception part of the MIMO CDMA system, user data are detected by photo-detectors and then the

operation of spreading by the same code of each user and finally the use of V-BLAST receiver to extract data user.

The following figure shows a simplified diagram of the receiver part of CDMA optical network based on electrical encoders. Indeed, to achieve the dialogue between source node and receiver nodes we choose CDMA techniques to make the routing of electrical signal from source to destination, this routing is done in classical ONOC with waveguide switching in the channel, our method let as make the routing in the electrical part of the system with giving each source node one code and the receiver node which have this code can receive the decode of the desired signal.

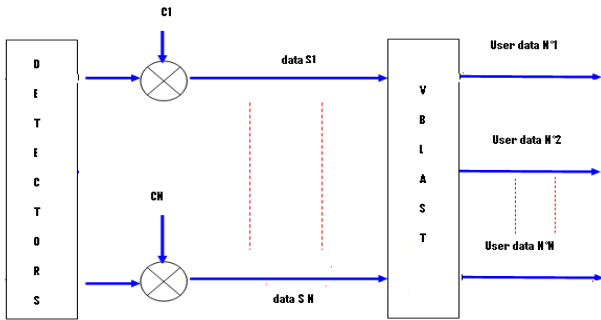


Fig. 10. The receiver part.

Principle of receiving algorithm

The V-BLAST algorithm has been discussed in details elsewhere [28], [29]. Here, we describe its main points for completeness and in order to introduce notations. The code VBLAST (Vertical Bell Laboratory Layered Space-Time) is based on a set of symbol blocks. We have in this case N_t blocks where each block is modulated by amplitude modulation, so with N_t symbol blocks, each block is sent to one of N_t lasers.

VBLAST algorithm can be described as the following: Preliminary_step: scheduling powers of vector components received.

Assuming that $\{k_1, k_2, \dots, k_{N_t}\}$ is the optimal detection order, then we can write:

$$SNR(s_{k_1}) \geq SNR(s_{k_2}) \geq \dots \geq SNR(s_{k_{N_t}})$$

Where $SNR(s_{k_{N_t}})$ denotes the SNR of the transmitted Component s_k of the vector s .

Step 1: Using the vector w_k annulling the decision is formed as y_k

$$y_k = w_k^T r_1 \tag{17}$$

Where $r_1 = r$ is the received vector.

Step 2: decide for y_k to obtain s_k

$$s_k = Q(y_k) \tag{18}$$

Where $Q(.)$ denotes a quantization operation, following the constellation used.

Step 3: Subtract symbols already detected the received vector:

$$r_2 = r_1 - s_k(H)_k \tag{19}$$

Where $(H)_k$ is the column k of the channel matrix H . The process is then repeated until the detection of the symbols.

The calculation of the vector canceling depends on detection criterion selected. The most commonly used criteria are the following:

- ✓ The standard zero-forcing (zero forcing: ZF).
- ✓ The criterion of minimizing the mean squared error (MMSE).

E. Comparative analysis of the performance of strict codes

For simulating the performance of MIMO CDMA system, we implement the V-BLAST detector and we study with computer simulation the performance of different configuration.

✓ *Performances of a 4x4 ONOC MIMO system with and without noise*

In this section, we study a 4x4 MIMO system of an ONOC architecture presented previously with strict code described above:

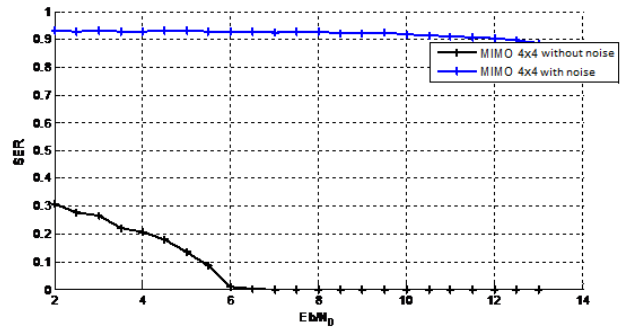


Fig. 11. Comparison of a 4x4 MIMO system with and without noise.

The previous figure shows the evolution of SER (Symbol Error Rate) based on signal to noise ratio of a 4x4 MIMO system.

From this figure, we see improving SER after removing AWGN. As done for the MIMO system with noise, we find that there's a lot of error and that is due to the inter-symbol interference between the co-channels.

For the MIMO system without noise, we see improved performance in terms of symbolic error rate. Note that for a noise equal to 6 dB signal was zero SER for MIMO

system without noise and SER about 0.9 for the system with noise.

✓ *Performances of 3x3 and 4x4 ONOC MIMO systems without AWGN*

In this section we are going to compare a 3x3 MIMO and 4x4 MIMO systems without AWGN.

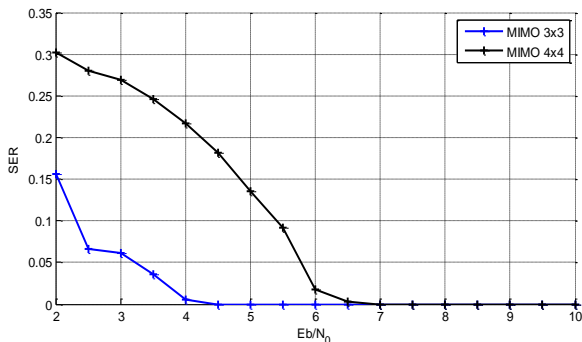


Fig. 12. Comparison of 3x3 and 4x4 MIMO systems without AWGN.

From the figure, we note that if the signal to noise ratio is increased, there are better SER. In addition, we note that the performance in terms of the SER 3x3 MIMO system is better than the 4x4 MIMO system and this up to interference inter-symbol in ONOC channel.

✓ *Comparison of 3x3 and 4x4 ONOC MIMO CDMA systems without AWGN*

In this section we introduce the CDMA concept, Instead of wavelength routing based on optical switch, we opt to a free space channel between source nodes and destination nodes, and the routing scheme is based on OOC code.

The comparison is made of two 3x3 and 4x4 MIMO systems.

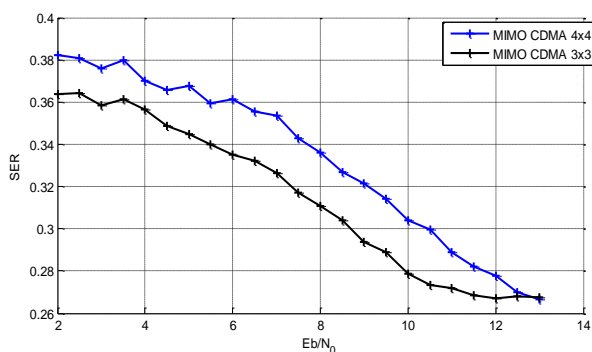


Fig. 13. Comparison of 3x3 and 4x4 ONOC MIMO CDMA systems without AWGN.

From the figure, we note that if the signal to noise ratio is increased, There are better SER, in addition we note that the performance in terms of SER 3x3 MIMO CDMA system is better than the 4x4 MIMO CDMA and this amounts to inter-symbol interference in MIMO

channel: the more to reduce the number of transceivers, the interference becomes less important which lead to a better bit error rate at the reception.

This figure show in one hand that if we increase the number of source nodes there's a degradation of the performances of the ONOC system, in the other hand, the figure show there's need to study the maximum number of source nodes in a miniature area.

✓ *Comparison of two 4x4 ONOC MIMO CDMA systems with and without and with AWGN.*

In this section, two 4x4 ONOC MIMO system is simulated with and without CDMA and AWGN.

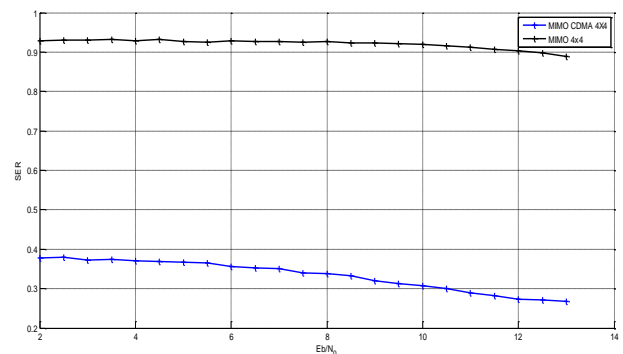


Fig. 14. Comparison of two 4x4 ONOC MIMO CDMA systems with and without and with AWGN.

We note from the figure above that ONOC MIMO CDMA systems are resistant to noise, which supports the usefulness of the concept in CDMA data security. According to both the figure, and condition of use of AWGN, the performance in terms of error rates symbolic MIMO CDMA system is better compared to the performance of MIMO system without CDMA.

This plot shows that CDMA technique has a good performance in the achievement of the dialogue between source nodes and destination nodes

4. Conclusion

In this paper, we present a new concept of on-chip optical networks based on MIMO (multiple input multiple output) systems. We model the channel of the optical system on chips and we have determined the transfer function of the channel with the help of two diffusers. Finally, based on assessment system as a communication system, we realize the simulation of bit error rate as a function of signal to noise ratio and we concluded that CDMA technique is a good method to achieve routing scheme between source nodes and destination nodes.

References

- [1] K. Ma, X. Li, M. Chen, X. Wang, *SIGARCH Comput. Archit. News*, **39**, 449 (2011).
- [2] S. Borkar, A. A. Chien, *Commun. ACM*, **54**, 67 (2011).
- [3] P. Sudeep, D. Nikil, *IPSI Transactions on system LSI Design Methodology*, **1**, 2 (2008).
- [4] D. A. Miller, *Proc. IEEE*, **97**, 1166 (2009).
- [5] A. Krishnamoorthy, R. Ho, X. Zheng, H. Schwetman, J. Lexau, P. Koka, G. Li, I. Shubin, J. Cunningham, *Proceedings of the IEEE*, **97**, 1337 (2009).
- [6] R. T. Chang, S. Member, N. Talwalkar, S. Member, C. P. Yue, S. S. Wong, *IEEE J. Solid-State Circuits*, **38**, 834 (2003).
- [7] G. I. Papadimitriou, C. Papazoglou, A. S. Pomportsis, *Lightwave Technol.* **21**(2), 384 (2003).
- [8] O'Connor, *Proceedings of the international workshop system level interconnect prediction*, **79** (2004).
- [9] B. E. Little, H. A. Haus, J. S. Foresi, L. C. Kimerling, E. P. Ippen, D. J. Ripin, *IEEE Photonics Technol Lett.* **16**(6), 816 (2004).
- [10] S. Atsushi, F. Tatsuhiko, B. Toshihiko, *EICE Trans Electron.* **E85-C**(4), 1033 (2002).
- [11] Rouskas G., *Wiley encyclopedia of telecommunications*. John Wiley & Sons; 2001.
- [12] M. Briere, B. Girodias, Y. Bouchebaba, G. Nicolescu, F. Mieyeville, F. Gaffiot, et al. *Design, automation and test in Europe conference and exhibition*, 2007. p. 1–6.
- [13] L. Zhang, M. Yang, Y. Jiang, E. Regentova, *Computers and Electrical Engineering, Comput Electr.*(2009), doi:10.1016/j.compeleceng.2008.09.010.
- [14] Balac Stéphane, *FOTON ENSSAT de Lannion Université de Rennes 1*.
- [15] Atef Allam, Ian O'Connor, Alberto Scandurra, 978-1-4244-5309-2/10©2010 IEEE.
- [16] G. F. Fan, R. Orobtcchouk, J. M. Fédéli, *Proc. SPIE 7719, Silicon Photonics and Photonic Integrated Circuits II*, 77190F, May 17, 2010.
- [17] Forget Sébastien, *Cours, Exercices et exemples d'applications*.
- [18] J. Alda, *Encyclopedia of Optical Engineering*, DOI:10.1081/E-EOE120009751,2003.
- [19] Tasso R.M.SALES, Donald J.Schertler, *RPC, RPC photonics, Inc, Newyork*.
- [20] Luminic optics. <http://www.luminicco.com>.
- [21] RPC photonics. <http://www.rpcphotonics.com/>.
- [22] J. A Salehi et al, *IEEE, Transactions on Communications*, **37**, 834 (1989).
- [23] Naoufal M. Saad, *Rapport de thèse Faculté de science Université de Limoges*, Mai 2005.
- [24] Ryah Fuji-Hara, Ying Miao, *University Of Tsukuba, Japan*.
- [25] Mohammed M. Alem-Karladoni, *article*.
- [26] T. L. Alderson, *Canada*.
- [27] Mesa Ali Abu-Grief, *USA*, 2007.
- [28] G. D. Golden, G. J. Foschini, R. A. Valenzuela, P. W. Wolniansky, *Electron. Lett.*, **35**(1), 14 (1999).
- [29] G. J. Foschini et al., *IEEE J. Select. Areas Commun.*, **17**, 1841 (1999).

*Corresponding author: sofien_mhatli@yahoo.fr